

Computer-aided analysis of signals from a low-coherence Fabry-Perot interferometer used for measurements of biological samples

Marcin Mrotek, Jerzy Pluciński, and Małgorzata Jędrzejewska-Szczerska

Gdańsk University of Technology, Faculty of Electronics and Telecommunications,
Gabriela Narutowicza 11/12, Gdańsk, Poland

ABSTRACT

The aim of the study was to develop an automated computer-aided system for analysis of spectrograms obtained from measurements of biological samples performed with a low-coherence Fabry-Pérot interferometer. Information necessary to determine dispersion characteristics of measured materials can be calculated from the positions of the maxima and minima that are present in their spectra. The main challenge faced during the development of the system was reliable detection of these maxima and minima in the presence of noise, without requiring substantial user interaction, and with an acceptable computational complexity.

Keywords: spectroscopy, Fabry-Pérot interferometer, optical fiber

1. INTRODUCTION

The aim of the study was to develop an automated computer-aided system for analysis of spectrograms obtained from measurements of biological samples¹⁻⁵ performed with a low-coherence fiber-optic Fabry-Pérot interferometer.

An example of a spectrogram obtained from a measurement of an empty interferometer cavity is presented in fig. 1.

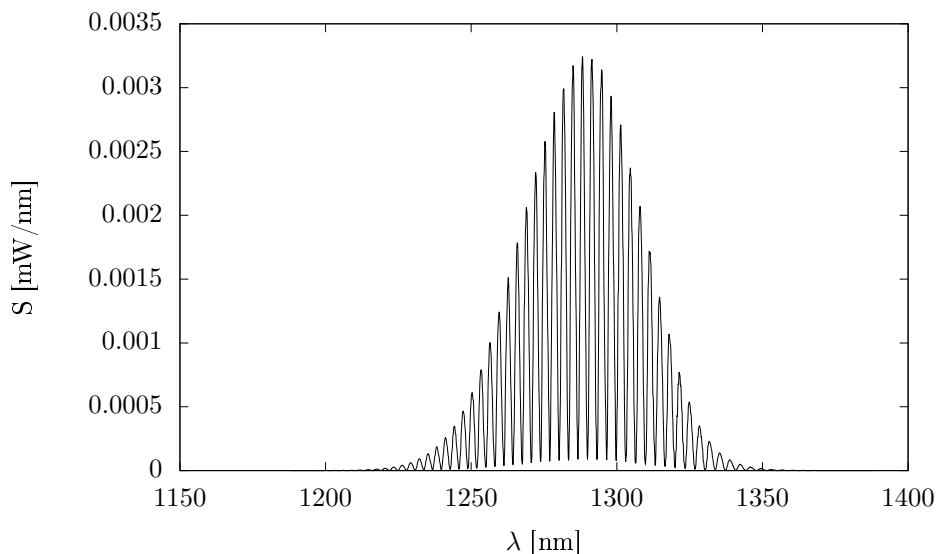


Figure 1. Example of a measured spectrogram used in analysis

Further author information: (Send correspondence to M.M.)

M.M.: E-mail: marcin.jan.mrotek@gmail.com

Spectrograms obtained from the performed measurements show a repeating pattern of maxima and minima, with the maxima corresponding to constructive interference in the interferometer cavity, and minima corresponding to destructive interference.⁷ Positions of these extrema can be used to determine the dispersion characteristic of the medium present in the cavity.

2. MEASUREMENT SETUP

The measurement setup presented in fig. 2 consists of a fiber-optic Fabry-Pérot interferometer, a low-coherence source, and an optical spectrum analyzer. To a first approximation, light propagating in the interferometer cavity (fig. 2) can be modeled with a planar wave. Due to a 180° phase shift⁶ upon reflection from the surface of the silver mirror, the wave reflected from the end of the optical fiber interferes constructively with the wave passing through the cavity for wavelengths satisfying the following equation:

$$2nL = \left(m + \frac{1}{2}\right) \lambda_{\max}, m = 0, 1, 2, \dots, \quad (1)$$

where n is the refractive index of the material filling the cavity of the interferometer, L is the geometric length of the cavity, and λ_{\max} is a wavelength at which the reflectivity of the interferometer attains maximum. The waves will interfere destructively for wavelength satisfying the equation:

$$2nL = m\lambda_{\min}, m = 1, 2, 3, \dots, \quad (2)$$

where λ_{\min} is a wavelength at which the reflectivity of the interferometer attains minimum.

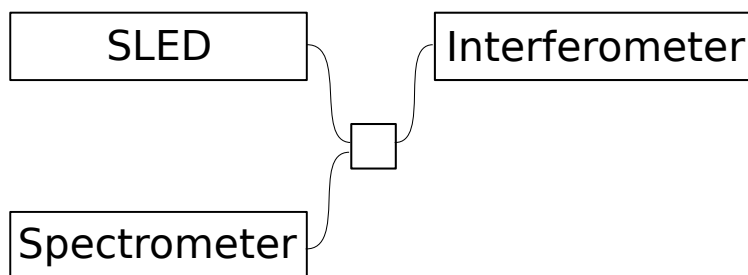


Figure 2. Measurement setup

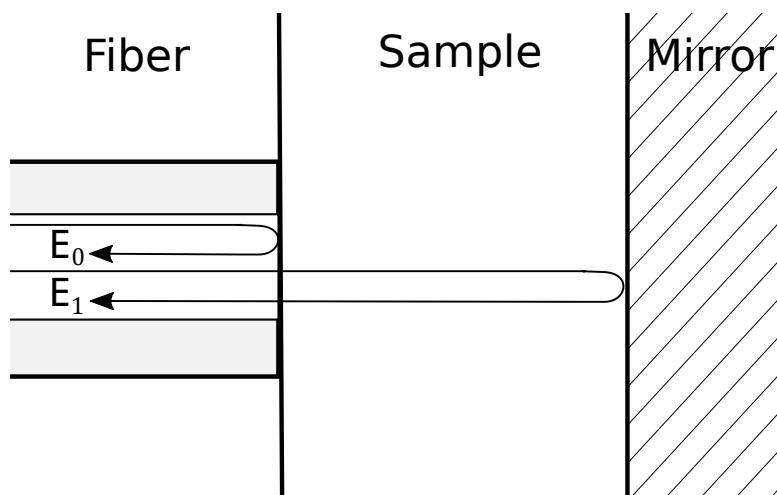


Figure 3. Interferometer cavity

3. CONSIDERED ALGORITHMS

The algorithm chosen for determination of the positions of maxima and minima of the spectrum should satisfy the following requirements:

- Detect the maxima and minima, in the presence of noise, with no false positives or negatives.
- Require minimal user interaction.
- Have low computational complexity.

The following algorithms were considered:

- Comparison of differences between consecutive maxima and minima against a given threshold.⁸ This algorithm finds spectral lines by comparing the distance between spectral maximum and minimum against a threshold selected by user.
- Using Fourier domain.⁷ This algorithm uses information obtained from the Fourier transform of the input spectrogram to determine approximate positions of the spectral maxima and minima and searches for extrema of the signal in the vicinity of these positions.

Peak detection by height comparison requires only one pass over the input spectrogram and does not require resampling, therefore its computational complexity is lower than the other method. The disadvantage of this algorithm is that it can result in false positives in presence of noise, or fail to detect peaks if the threshold value is chosen inappropriately. Therefore, this algorithm requires substantial user interaction, and has been discarded.

Fourier transform of the signal reveals the frequency of the modulation superimposed on the source spectrum. The transform has to be calculated from a signal resampled to the wavenumber domain, as spectral lines are not uniformly distributed in the wavelength domain, even in the ideal case of no dispersion.

There are thus two possible means of obtaining the transform:

- Nonuniform Discrete Fourier Transform.⁹ Discrete Fourier Transform can be calculated for a nonuniformly sampled signal, although the Fast Fourier Transform algorithm cannot be used, and the transform has to be calculated directly from the definition.
- Uniform DFT preceded by resampling.⁷ This method of calculating the Fourier transform requires an additional step in order to obtain a signal sampled uniformly in the wavenumber domain, but the FFT algorithm can be used afterwards.

The computational complexity of NDFT is quadratic in the general case, as opposed to $O(N \log_2 N)$ (where N is the number of samples in the input signal) complexity of FFT. For the sizes of data sets used in this analysis this complexity outweighs the cost of resampling, therefore the NDFT algorithm has been discarded.

3.1 Resampling

The resampling process has to preserve the total power of the signal, *i.e.* the integral of the signal under any portion of the spectrum. For two arbitrary wavelengths $\lambda_1 < \lambda_2$ and their respective wavenumbers $k_1 = \frac{2\pi}{\lambda_1}$ and $k_2 = \frac{2\pi}{\lambda_2}$, the original signal $f(\lambda)$ and the resampled signal $g(k)$ have to satisfy the following equation:⁶

$$\int_{\lambda_1}^{\lambda_2} f(\lambda) d\lambda = \int_{k_2}^{k_1} g(k) dk. \quad (3)$$

In particular, two consecutive samples in the wavelength domain, λ_1 and $\lambda_1 + \Delta\lambda$ (where $\Delta\lambda$ is the sampling interval) have to satisfy equation:

$$\int_{\lambda_1}^{\lambda_1+\Delta\lambda} f(\lambda)d\lambda = \int_{\frac{2\pi}{\lambda_1+\Delta\lambda}}^{\frac{2\pi}{\lambda_1}} g(k)dk, \quad (4)$$

which, if the signals are approximated with step functions, reduces to

$$g\left(\frac{2\pi}{\lambda_1}\right) = f(\lambda_1) \frac{(\lambda_1 + \Delta\lambda)\lambda_1}{2\pi}. \quad (5)$$

Following this transformation, the distances between the signal's samples can be uniformized. In general case, for a given window function $w(k)$, the resulting series of samples $h[i]$ can be obtained from the original signal $f(\lambda)$ using equation (5) as follows

$$\begin{aligned} h[o] = h(k_0 + o\Delta k) &= \sum_{i=i_1}^{i_2} g\left(\frac{2\pi}{\lambda_0 + i\Delta\lambda}\right) w\left(k_0 + o\Delta k - \frac{2\pi}{\lambda_0 + i\Delta\lambda}\right) \\ &= \sum_{i=i_1}^{i_2} f(\lambda_0 + i\Delta\lambda) \frac{(\lambda_0 + (i+1)\Delta\lambda)(\lambda_0 + i\Delta\lambda)}{2\pi} w\left(k_0 + o\Delta k - \frac{2\pi}{\lambda_0 + i\Delta\lambda}\right), \end{aligned} \quad (6)$$

where λ_0 is the initial wavelength of the original spectrogram, k_0 is the initial wavenumber of the resampled spectrogram, Δk is the sampling interval of the resampled spectrogram, $h[o]$ are the samples of the resampled spectrogram, $w(k)$ is the window function, and i_1, i_2 are the indices of samples of the original spectrogram where the window function takes nonzero values (calculated based on the current sample index in the resampled spectrogram and length of the window function). As the length of any practical window function is significantly lower than the size of the input data and does not directly depend on it, this algorithm can be considered to have linear algorithmic complexity.

Lanczos window (fig. 4) was chosen for the purpose of interpolation, as it is a commonly used resampling function.¹⁰ The Lanczos window is defined as a family of functions indexed by a shape parameter a :

$$w'_a(x) = \begin{cases} \text{sinc}(x)\text{sinc}\left(\frac{x}{a}\right) & \text{for } x \in [-a, a] \\ 0 & \text{for other } x \end{cases}, \quad (7)$$

where $\text{sinc}(x) = \frac{\sin(\pi x)}{\pi x}$.

To use this window with wavenumber values, the sample positions can be scaled by the sampling interval:

$$w_a(k) = w'_a\left(\frac{k}{\Delta k}\right). \quad (8)$$

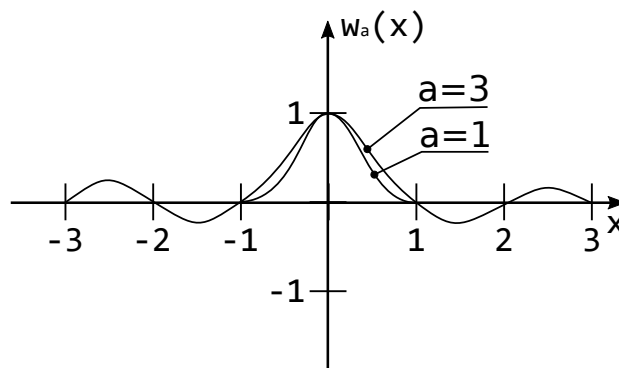


Figure 4. Lanczos window function used in the resampling process

3.2 Fourier domain

A Fourier transform of an input spectrogram corresponds to an interferogram of the measured signal as a function of optical path length. An example of a Fourier transform of a measured spectrogram is presented in fig. 5

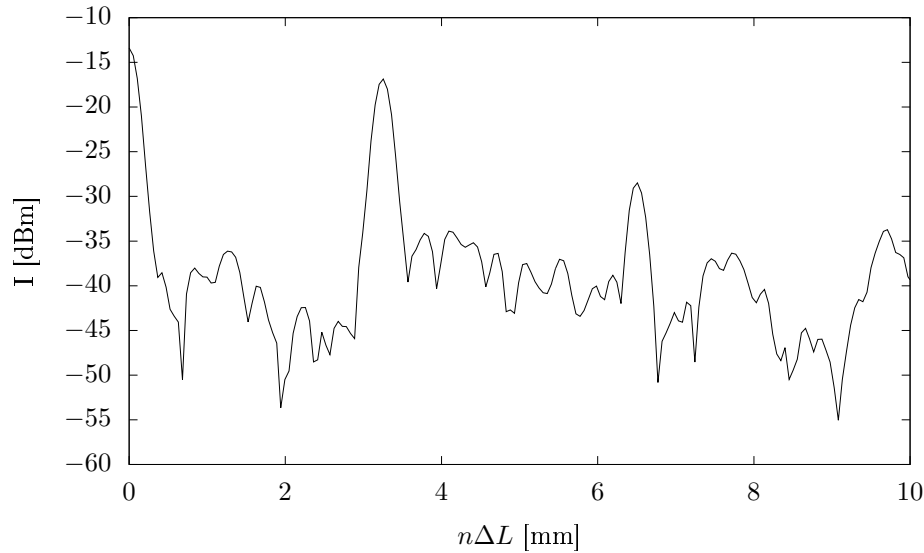


Figure 5. Fourier transform of the spectrogram presented in fig. 1, in lin-log scale

The second peak in the Fourier transform of the spectrogram corresponds to the mean optical path length difference between the interfering waves $2n\Delta L$, and thus the base frequency of the modulation present in the spectrum. Position of this peak can be obtained by finding the point with maximum difference between its height and the minimum of the signal up to that point. Afterwards, this information can be used to divide the original into equal parts of length $\frac{\pi}{n\Delta L}$, and to find the maxima and minima of these parts.

3.3 Dispersion characteristics

Transforming equation (1), the order of interference of each maximum can be obtained as follows

$$m'_i = \frac{2nL}{\lambda_i} - \frac{1}{2}, \quad (9)$$

where m'_i is the approximate order of interference of i th maximum, and λ_i is wavelength of i th maximum.

Assuming that these numbers should be consecutive and decreasing, after finding the index i_{best} such that $m'_{i_{\text{best}}}$ is closest to an integer, the integral orders of interference can be calculated as follows

$$m_i = i_{\text{best}} - i + [m'_{i_{\text{best}}}], \quad (10)$$

where $[.]$ denotes the nearest integer number.

Using equation (1) again, and assuming that geometric length L of the interferometer cavity is known (it can be obtained by taking a measurement with empty cavity, and assuming the refractive index of air to be equal to 1), the dispersion characteristics of the material in the cavity of the interferometer can be calculated as follows:

$$n(\lambda_i) = \frac{1}{2L} \left(m_i + \frac{1}{2} \right) \lambda_i. \quad (11)$$

Positions of the spectral minima and equation (2) can be used in a similar manner to obtain more data points.

4. RESULTS

Comparison of calculated and expected dispersion characteristics of free air is presented on fig. 6. The discrepancy from the expected constant index of refraction equal to 1 results from the difference between the positions of maxima in the intensity of received light and the maxima of the reflectance of the interferometer. As a source with Gaussian spectral characteristics was used, the maxima of received intensity are shifted by the slopes of the input spectrum. The relative error does not exceed 0.06%, and is deemed acceptable.

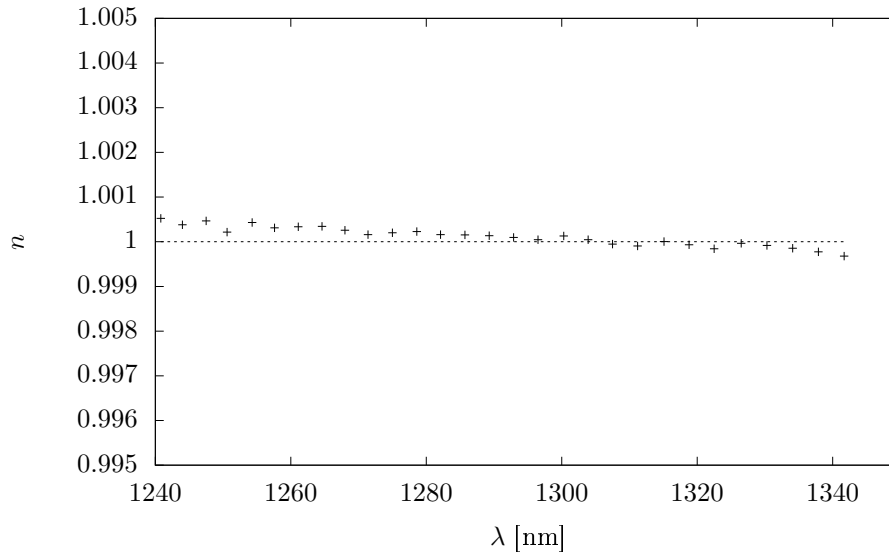


Figure 6. Calculated (points) and expected (line) dispersion characteristics of an empty cavity

5. CONCLUSION

A computer-aided, fully automated system capable of determining the dispersion characteristics with relative error no higher than 0.06% has been developed. Further studies can be undertaken to improve the accuracy of results. Possible improvement can be achieved by taking into account the effects of non-flat spectral characteristics of the source, Gouy phase shift, and coupling coefficients between the optical fiber and interferometer cavity, although these methods introduce additional computational complexity.

ACKNOWLEDGMENTS

This study was partially supported by the National Science Centre, Poland under the grant No. 2011/03/D/ST7/03540, as well as DS Programs of the Faculty of Electronics, Telecommunications and Informatics of the Gdańsk University of Technology.

REFERENCES

- [1] P Wierzba, M Jędrzejewska-Szczerska, "Optimization of a Fabry-Perot Sensing Interferometer Design for an Optical Fiber Sensor of Hematocrit Level", *Acta Physica Polonica*, A. 124 (3)
- [2] K Karpienko, M Gnyba, D Milewska, MS Wróbel, ..., "Blood equivalent phantom vs whole human blood, a comparative study", *Journal of Innovative Optical Health Sciences* 9 (02), 1650012
- [3] D Milewska, K Karpienko, M Jędrzejewska-Szczerska, "Application of thin diamond films in low-coherence fiber-optic Fabry Pérot displacement sensor", *Diamond and Related Materials* 64, 169-176
- [4] D Majchrowicz, M Hirsch, P Wierzba, M Bechelany, R Viter, ..., "Application of Thin ZnO ALD Layers in Fiber-Optic Fabry-Pérot Sensing Interferometers", *Sensors* 16 (3), 416

- [5] *Biosensors for Security and Bioterrorism Applications*, Dimitrios P. Nikolelis, Georgia-Paraskevi Nikoleli, [ed], 2016 Springer
- [6] M. Born, E. Wolf, *Principles of Optics (7th (expanded) edition)*, Cambridge University Press 2006.
- [7] J. Goodman, *Statistical Optics*, Wiley Classics, 2000
- [8] "Find local maxima", (accessed 27.06.2016). [<http://www.mathworks.com/help/signal/ref/findpeaks.html>]
- [9] F. Marvasti, *Nonuniform sampling: Theory and Practice*, Plenum Publishers Co., 2001
- [10] K. Turkowski, S. Gabriel, "Filters for Common Resampling Tasks", *Graphics Gems I*. Academic Press. pp. 147–165. 1990.